Development of an Open System for Evaluating Material Charging Characteristics from Industrial Waste Heat

Jack Reynolds[1], Jonathon Elvins[1] Eifion Jewell[1] and Justin Searle[1]

1 Swansea University, Swansea (United Kingdom)

Abstract

The current research tackles the energy trilemma, capture, storage, and re-use of industrial waste heat (IWH) by presenting the development of a laboratory-scale charge analyser for thermal storage (CATS) utilizing thermochemical materials (TCMs). The purpose of the study is to evaluate a material's charge performance relative to the reactor's capabilities. The temperature, flow rate, and material quantity are altered to generate an operational window. The reactor has been designed to work as an open system, whereby the IWH stream will pass directly through any TCMs under consideration. For this study, silica gel was chosen as the material for commissioning the reactor as it is well understood from a mass loss perspective and its relative ease of material preparation. The reactor can produce temperatures between 50-650°C and flows in the region of 200-900 l/min. During experimentation we can record the mass change (resolution 0.01g) up to a maximum of 10.2kg, temperature changes up to a maximum of 1100°C, and flows (between 0.2-25m/s).

Keywords: Industrial Waste Heat, Silica Gel, Thermochemical Materials

1. Introduction

With the exhaustion of our world's main fossil-based energy resources and the continued worsening of our environmental conditions in the past decades, it is vital we look to change the way we generate, use, and store our energy. For most of the industrial sector, heat energy is used in some way or another for manufacturing of the desired products. The heat energy is subsequently discharged from the process through thermal carriers such as gases or liquids and vented to atmosphere or discharged into local bodies of water. U.S. department of energy reported that between 20 to 50% of industrial energy input is lost as industrial waste heat (IWH) (BCS INC, 2008). Depending upon the process, IWH can be discharged over a large temperature range, however the majority of heat sources are below 200°C except for the Iron and Steel sector where the range is 200-1000°C (Papapetrou et al, 2018). This is highlighted in Figure 1. The inherent problem with utilising IWH can be its economics of recovery, discontinuous nature and the distance mismatch between the source and the end use. The solution to both these problems is effective heat storage.

Thermal energy storage (TES) is considered among passive IWH recovery technologies and could potentially fill the gap between energy supply and demand. Application of TES for IWH recovery could reduce investment cost, improve the capacity factor and reduce start-up and partial load losses in industries (Miró et al, 2016; Brueckner et al, 2014)

TES can be classified as sensible heat storage (SHS), latent heat storage (LHS) and thermochemical heat storage (TCS). SHS in comparison with other technologies is a simple, low-cost, and mature technology however is associated with inferior energy density and considerable storage volumes (Sunku Prasad et al, 2019). LHS offers greater energy density in comparison over the same temperature gradient, however LHS has some characteristic drawbacks such as corrosion and leakage. Both SHS and LHS are not suitable for long term application as heavy insulation is required to minimize typical energy leakage. (Wu et al, 2019; Fumey et al, 2019). TCS can store the energy at wide range of temperatures based on chemical bonds of suitable materials with minimum energy loss for long term application and higher associated energy storage density (Lin et al., 2021).

Sorption heat storage has been utilized for both mobile THS, transporting IWH to an off-site heat demand, and for inter-seasonal heat storage at the demand location (Krönauer et al., 2015; Sutton et al., 2018). For the lower end of IWH (<200°C) various salt hydrates could be suitable such as $CaCl_2$, $LiNO_3$ and $SrBr_2$ (Sutton et al.,

doi:10.18086/eurosun.2022.13.18 Available at http://proceedings.ises.org

2018; Salviati et al., 2019). For the higher end of IWH, there are far less options in terms of materials and research is scarce in comparison. Two stand out materials that have been studied are $Mg(OH)_2$ (Zamengo et al, 2015) and $Ca(OH)_2$ (Funayama et al, 2019) which are suitable for temperatures above 350°C and 550°C respectively.

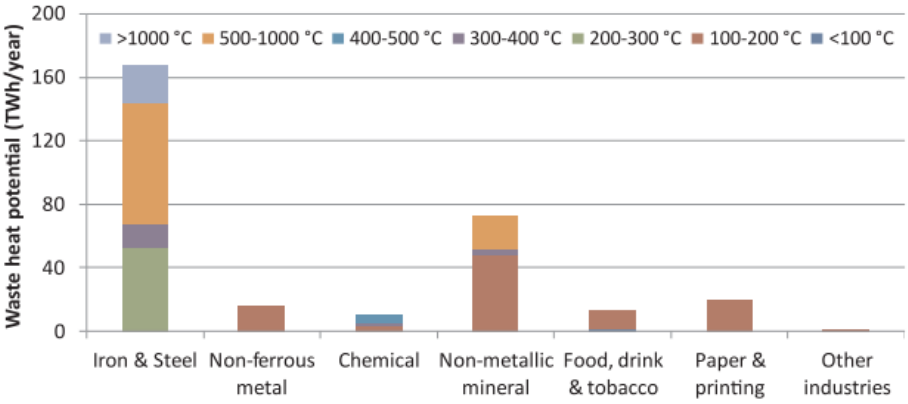

Fig. 1: Waste heat potential per industrial sector and temperature level for EU industry in 2015 (Papapetrou et al, 2018)

The aim of this work is to design and commission a reactor to assess the charging performance of various materials within the range of the reactor's capabilities of representing IWH. This will allow for decisions to be made on which material is best suited to a particular IWH stream. Here we will alter temperature, flow, and material quantity to produce an operational window. The reactor has been designed to work as an open system, whereby the IWH stream will pass directly through any TCMs in a fixed bed. The storage of the material in the reactor has been designed so it can be easily removed for transport. For this study, silica gel was chosen as the material for commissioning the reactor as it is well understood from a mass loss perspective and its relative ease of material preparation.

2. Design and Build of the Reactor

The performance of any materials selected for use in storage of IWH need to be assessed in a lab-scale reactor. To do this, the charging performance of a material should be assessed in terms of its resident time to become fully dehydrated at a given temperature and flow. In this work, the design and optimization of a charge analyser for thermal storage (CATS) capable of mimicking the flow of industrial waste heat on a lab-scale over a broad range of temperatures and flows in the low-medium temperature range is shown.

2.1. Reactor Requirements

Incorporating as many measurements as possible into a RIG is essential to giving a more accurate judgement and a better understanding of what is transpiring. To validate the discharge performance of the TCM, there are a couple of parameters to suggest the resident time required. These are as follows:

- Change in Mass
- Change in Temperature

For the replication of the IWH, a heat source is required that can provide the range of temperatures covered in the low-medium range (100-700°C) with the ability to easily control and monitor the temperature and the flow rate. An open structure with the ability to contain TCMs is needed with following necessities:

- Allow incorporation of sensors
- Ability to withstand heat
- Limit the amount of heat lost to the environment
- Allow flow of IWH through material
- Easy to remove and add materials

2.1.1 Mass Measurements

Accurately measuring mass of TCMs is the most accurate way of judging what state the salt is in. If a known quantity of salt is contained within a matrix, any additional weight gained can be attributed to absorbed water. By applying heat, this water can be removed and by weighing in stages it is possible to observe progress along a charging profile. However, this is not ideal in any situation for two reasons. First it is not possible to monitor the mass over time for a complete cycle with live results, and secondly, the act of removing the salt from the heat in normal conditions will affect the actual water content. To avoid this, we need to have mass measurements while heat the is being applied. The solution to this is to measure the whole RIG in which the SIM is contained. An example of this is shown in the work by Zamengo et al. (2015) where the packed bed reactor is sat on an electronic balance. To achieve this the electronic balance needs to have a high maximum load to allow for the weight of the RIG, while also have a high accuracy to account for the low mass changes occurring during the reaction. On top of this a data logging function is required so the mass can be monitored throughout experimentation.

2.1.2 Temperature Measurements

Temperature measurements need to be taken in the RIG for three reasons. The first is to monitor the temperatures coming from the IWH heat source are as expected. Secondly, we need to understand how much heat energy is being lost from the point of heat source to the location of our storage materials. Lastly, the temperature changes that may occur before and after the thermochemical materials (TCMs) need to be monitored which may give an indication of how far along the charge cycle progression is. The heat energy from the IWH stream should in theory be absorbed by the TCMs, breaking the bonds between the water molecules and the material in question. This should result in the temperature of the air stream being reduced at the outlet compared to the inlet. This continues until the salt reaches its anhydrous state or reaches a stable salt hydrate at a given temperature. At this point there should be a limited difference between the inlet and outlet, giving us an indication that the charge cycle is complete. The requirements of the thermocouples (TCs) are as follows. They need to be able to withstand the maximum temperature that may be subjected to the materials in the RIG. They will also need datalogging capabilities so the temperatures can be monitored throughout the charging profile.

2.1.3 IWH Source

The heat source itself needs to cover the range of temperatures most associated with IWH sources (Low/Medium Temperatures). This needs to be accurately controlled while also considering the flow of air. Safety of the device is the biggest concern, and there cannot be any risk of overheating, damage, or cause any harm in the close vicinity.

2.1.4 Apparatus to Hold TCMs

The materials utilised in the apparatus to hold the SIM and any other components involved in the RIG need to handle the temperatures that are capable from the chosen waste heat source replica. There needs flexibility of within the piping to allow separation of the RIG from the heat source to prevent impacting upon the mass measurements. The RIG should be insulated where possible to limit the amount of heat lost the environment. The RIG should include an easy to remove compartment for the materials so that they can be transferred to an alternative discharge unit. There needs to be small access points incorporated for any sensors that will be fitted into the RIG.

2.2. Reactor Design

Following all the design requirements mentioned above, the finalised reactor design is shown in Figure 2. The heat source is a Leister Hotwind System hot air blower. This is commonly utilised in continuous drying,

shrinking, and coating processes. The continuous nature makes it ideal for use as our IWH source, aswell as having control over temperature and flow between 50-650°C and 200-900 l/min respectively. To have even more control over temperature, the Leister CSS is incorporated and programmed to control the temperature from an external TC. This allows the required temperature to be set in the inlet of the RIG as opposed to within the air blower. The Hotwind System is also fitted with an alarm contact and combined with a fabricated alarm we can prepare for any situation where the air blower might be overheated. The entire system is then fixed to an adjustable platform to allow for any change in height while also preventing movement during experimentation.

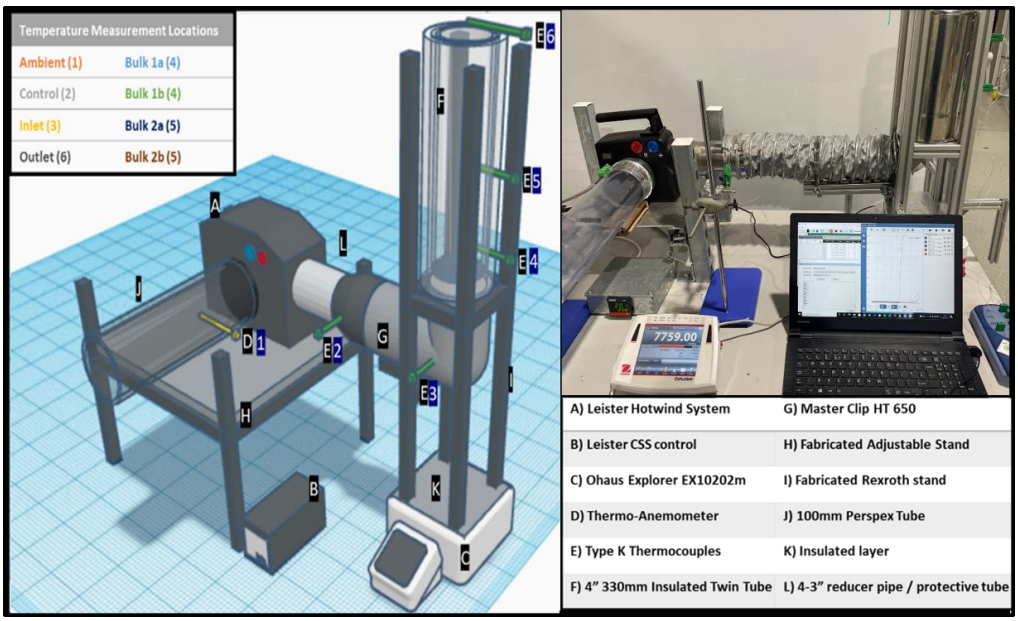

Fig. 2: 3D model of the lab-scale CATS highlighting all key components and locations (Left). Experimental set up (Right).

The main element of the RIG is the insulated twin tube with measurement adapters fitted in the side. The length of the tube is 330mm and the inner diameter (ID) is 100mm. The outer diameter is 150mm with 25mm of insulation held between the two stainless-steel tubes. Within this there is a removable stainless-steel tube with a perforated based capable of holding the testing TCM. The diameter of this tube is 94mm. This tube has holes present in the side that line up with the measurement adapters for incorporated sensors. The twin tube is then enclosed within a fabricated rexroth stand to allow for the elevation needed to fix the flexi tube underneath. This tubing is made from a flexible two-ply spiral hose made of heat-resistant fabric and steel spiral which is resistant up to temperature of 650°C. This has ID of 105mm and strapped to the inner twin tube by a SS jubilee clip. The flexibility of this piping allows for change in mass measurements during experimentation. To form a seal between the rig and the Hotwind, the tubing is strapped to a 4-3-inch reducer tube which has been welded to the protective tubing attachment of the Hotwind. The reducer tube has been fitted with holes for the control TC.

With a sufficient seal between the heat source and the RIG, the flow rate can be monitored prior to the hotwind to avoid the need of heat resistant flow sensors. To do this a 100mm Perspex tube has been fixed to the filter attachment of the hotwind. With a known diameter of the pipe and the flow speed, the flow rate through the RIG can be calculated. The air speed is monitored using a hot wire CFM thermo anemometer and datalogger. This system is capable of measuring air velocity between 0.2-25 m/s using a simple probe that can be inserted into the stream. As well as air velocity, the probe can measure temperatures up to 50°C. As this probe is located prior to the heat source, we can use this to simultaneously record the ambient temperature during the reaction. The rexroth is placed on top of a Ohaus Explorer EX10202m scale capable of measuring masses up to 10.2kg with a readability of 0.01g. The Ohaus scale connects with the Ohaus SPDC Data Collection software to send mass recording at desired intervals during the charge cycle. The scale itself is only operational to temperatures of 40°C. To prevent any heat transfer between the RIG and scale, a thin insulating layer is placed between the scale and the rexroth stand.

Type K TCs with 310 stainless steel sheath and a maximum operating temperature of 1100°C are used for temperature measurements through the RIG. The first two TCs are placed in the reducer tube just prior to Hotwind nozzle. One of these feeds straight to the CSS temperature control and the other to the data logger. At the end of the flexi pipe, just before reactor, a TC is placed and selected as the inlet temperature. In both measurement adapters, two TCs are placed with the aim of one being at the pipe centre and second close to the pipe walls. These are our bulk temperature recordings. The last TC is placed above the exit stream of the RIG and is the outlet temperature recording. All these TCs are connected to a Pico logger TC-08 which transfers the live temperature recording to the Pico data collecting software.

The CATS offers an ability to screen materials for use in THS. With this set-up an estimate a recharge efficiency is possible and any alterations to conditions and system design to best match the material under consideration can be done. Once operational windows are found, IWH sources can be targeted for capture within that range.

3. Material Preparation

Silica gel was chosen as the material for commissioning the CATS system as it is well understood from a mass loss perspective and the relative ease of material preparation. To add moisture evenly to the silcia gel, a Memmert constant climate chamber HPP110eco is used. Inital static vapor sorption (SVS) tests were first carried out at three different RH% values all at 25°C (Figure 3). 3 petri dishes, each containing 10g of Silica gel were located in a sealed chamber with controlled local relative humidity and left for 168 hours to assess the maximum water uptake. The maximum values were generally achieved within the first 24-48 hours showing no further uptake over the remaining test duration. The results show different maximum moisture uptake for different conditions and as such it is key to keep synthesis conditions the same if consistent discharged material is to me made. As the investigation will focus upon fully hydrated silica gel, 25°C and 75% RH are the conditions choosen for material synthesis.

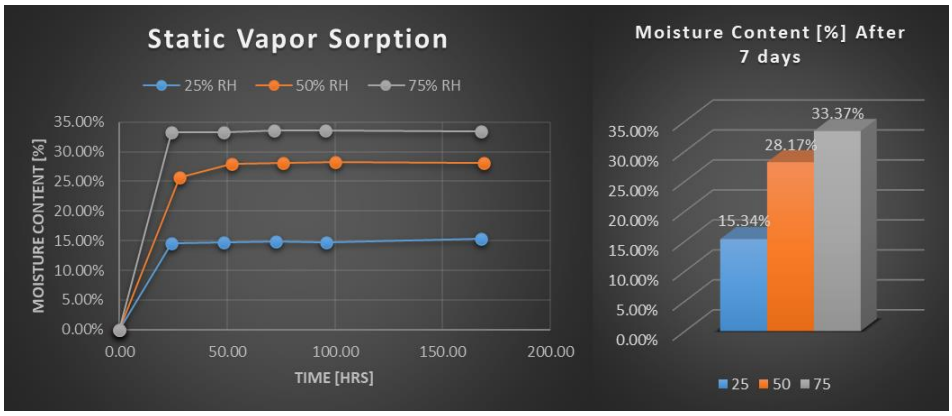

Fig. 3: Static vapor sorption (SVS) of 10g of Silica gel at 25°C at 25%, 50%, and 75% relative humidity (Left). Moisture content after 7 days (Right).

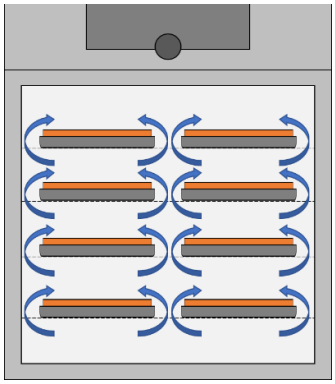

Fig. 4: Loading of Silica Gel in the Memmert constant climate chamber HPP110eco for large scale material preparation.

For bulk hydration, 300-400g of dry silica gel is loaded onto trays (32 x 23 cm) allowing for a thin layer of material to improve water uptake. Eight trays are then loaded into the climate chamber allowing for adequate air flow (Figure 4). At initial loading, the RH% of the oven drops due to rapid water uptake. Over the next 48 hours, this value equilibriates towards the set value. Once this is achieved it is possible to spot test the material and assess the moisture content. To do this a Ohaus MB120 moisture analyser is used. 5g of silica gel is subject to 200°C static drying with switch off criteria set to 1mg change over 120 seconds. If the moisture content is >33%, hydration is considered complete and materials are stored for use in the CATS.

4. Reactor Operation and Data

Example data received from the CATS is shown in Figure 5. The key indicators for duration of reaction come from the mass and temperature data. There is a steady loss of mass over time that flattens out when the charge reaction is deemed complete. This generally coincides with the outlet temperature that plateaus around its maximum observed value. The average flow data is used to show if there is any sudden change in the fixed bed during reaction and this, combined with the total reaction time proposed by the mass and temperature value, can give an estimate of the total energy used during the charge reaction. Any alteration to the IWH conditions, reactor design, and quantities of material used will change the energy required to charge the material set. With this data an operational window for silica gel to be used as an industrial waste heat storage material is defined

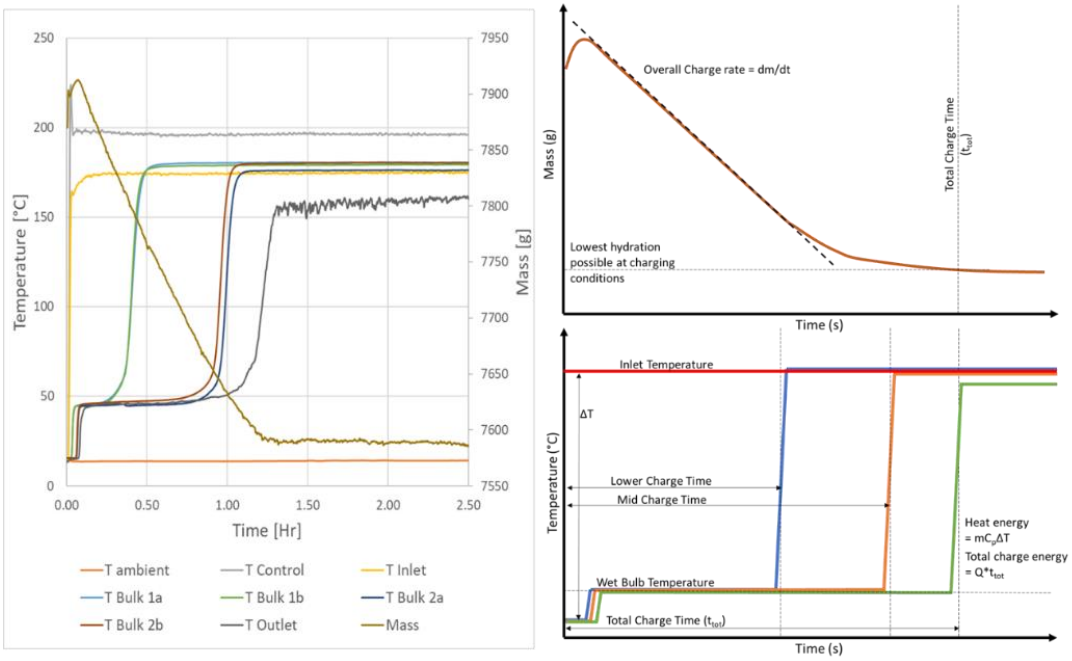

Fig. 5: Example data received from the CATS for silica gel at 200C set temperature and flow 7 set fan speed (Left). Data to be collected from the CATS (Right).

4.1. Air Speed to Mass Flow

As mentioned above a single point of measurement will be used to record air speed during experimentation, however the flow of air in a circular duct is not evenly spread across the plane of the duct. This is because of the friction that occurs at the duct walls that ultimately reduces the flow compared to the centre, creating the parabolic profile shown in Figure 6. Any obstruction such as fans, corners, duct fittings, tees, and coils all create turbulence in the duct, further changing the velocity over the cross section. To reduce the amount of turbulence, readings should be taken 7 duct diameters downstream and 1 and ½ upstream of any flow disturbance. For a round duct, the equal-area method should be used, whereby the air speed is taken at the centre of equal concentric areas and averaged. Figure 6. shows this where by two entry points, perpendicular

to each other, allow reading points to be taken vertically and horizontally through the centreline. An alternative method of obtaining the average flow is to take a measurement at the centre and multiple this by 0.9 (TSI Airflow, 2014). This can achieve an accuracy of +/- 5%. As the Thermo-Anemometer will remain central in the duct during experimentation, a comparison on the data received from the central data point and the traverse method is required to decide a multiplication factor the CATS system going forward.

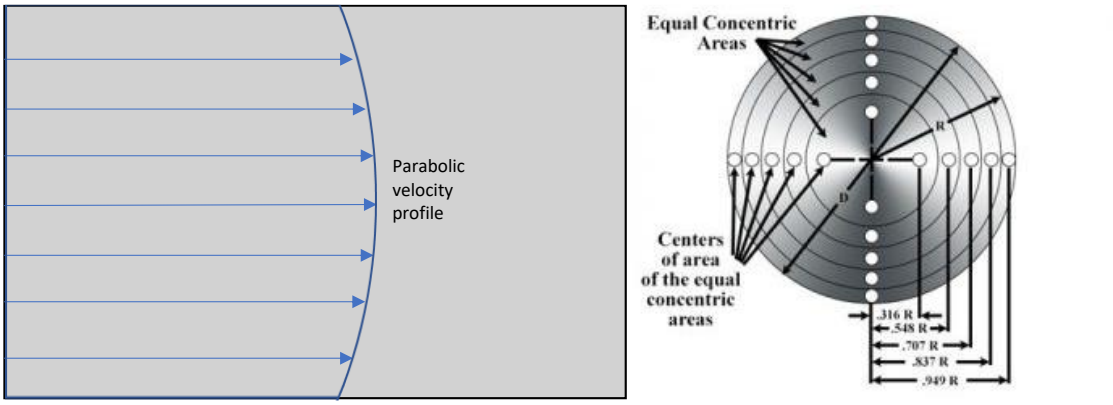

Fig. 6: Graph showing Actual Flow Rate vs Flow Setting varying Position, Temperature & Material.

Tab. 1: Results from air flow approximation experiment comparing central measurement point and traverse method at room temperature for flow setting 4 and 7.

Flow Setting 4		**Flow Setting 7**	
Method	**Air Speed [m/s]**	**Method**	**Air Speed [m/s]**
20 Point Traverse Method	1.40	20 Point Traverse Method	1.76
0.9 x Central Method	1.37	0.9 x Central Method	1.77
% Difference	1.68%	% Difference	0.69%

For each air speed measurement, the sensor was set in place and 30 data points were taken over 5 minutes (10s increments). The average of these values was then calculated as an input into table 1. The Traverse method was conducted over two different operational flow rates. For both sets of experiments the 0.9x Central Method was well within the quoted 5% difference of the 20 Point Traverse Method. This validates that a single point of flow measurement is sufficient to record during each experiment and a simple multiplication factor of 0.9 can be used to correct this.

To calculate the air mass flow (μ_{av}) the following equation can be used:

$$\mu_{av} = \nu \times CSA \times \rho_{air} \times 3240 \qquad \text{(eq. 1)}$$

- ν – Average Air Speed [*m/s*]
- CSA – Cross-sectional Area [m^2]
- ρ_{air} – Air Density [kg/m^3]
- 3240 – Multiplication factor for speed variation over a circular duct and to convert from units of seconds to hours.

4.2. Mass Measurement

To validate the scale's ability to record a mass change while connected to the flexi pipe, an experiment is set up to record the mass value of known weights. Four weights were chosen for this spread over a typical range expected from TCM mass losses. These are 74.80g, 118.9g, 125.27g & 191.32g. Each weight was placed on the scale 3 times at two different locations (Top and Base) and an average of the values calculated. The results from this are shown in Table 2. For all the results, the mass recorded was within 1% difference to the actual value. There is no significant trend suggesting this % difference changes when the mass of the object is changing. However, there is a difference in values from the mass measured at the base of reactor as opposed to the top of the reactor. All values at the base show a decrease in mass from the actual value, whereas all value at the top show an increase in mass from the actual value. This is considered to be an effect of the position of the weight in respect to the flexi pipe connection.

Tab. 2: Results from Scale Sensitivity Measurements

Mass at Base			**Mass at Top**		
Standard Mass	**Mass [g]**	**Av % Difference**	**Standard Mass**	**Mass [g]**	**Av % Difference**
1	74.8	0.77	1	74.8	-0.61
2	118.8	0.75	2	118.8	-0.57
3	125.3	0.77	3	125.3	-0.69
4	191.3	0.59	4	191.3	-0.33

The mass measurement is the first indicator of charge completion that results in a value of resident time (t_{rM}) used for total charge energy. Figure 5 shows that the mass linearly decreases for most of the charge duration before plateauing at its final 'dry' state. To obtain a residence time from this data, the gradient change during the reaction must be calculated. Using a selected 'end gradient' criteria, an exact time when the mass has levelled out to an appropriate state can be collected.

4.3. Temperature Measurement

The temperature is monitored at the system inlet to initially understand the heat loss in the distance between the Hotwind and the reactor. With knowledge of this we can then adjust the Hotwind temperature to get a desired temperature going through the material. This temperature reading subsequently allows comparison to all the other locations (Bulk1, Bulk 2, Outlet), assisting in defining charge completion at each point. Finally, the inlet is used to calculate the energy of the flow from the difference in temperature to ambient (25°C).

The loss of temperature in the flexi pipe between the heat source (Hotwind) and the reactor was investigated. The reactor was filled with a consistent amount of dry silica gel (1050g) and the Hotwind set at various flow settings and temperatures. The chosen flow settings were 4, 7, and 10. The chosen temperatures were 100°C, 200°C, and 300°C. For each experimental condition, the system was allowed to equilibrate for 10 minutes. 30 data points were subsequently recorded over 5 minutes and average values were calculated for the control and inlet TCs. The difference between these values is then labelled ΔT. The results are shown in Figure 7. Increasing the flow rate slightly decreases the loss of heat energy, however the largest losses occur through increases to the temperature. Generally, increasing the set temperature by 100°C increases the ΔT by around 20°C. Following this trend, selecting the Hotwinds maximum temperatures (650°C) and a maximum flow setting, temperature losses around 120°C would be expected, resulting in a maximum inlet temperature of around 530°C and flow speeds around 0.77 m/s. This is important to know when choosing TCMs with high charge temperatures for future experiments.

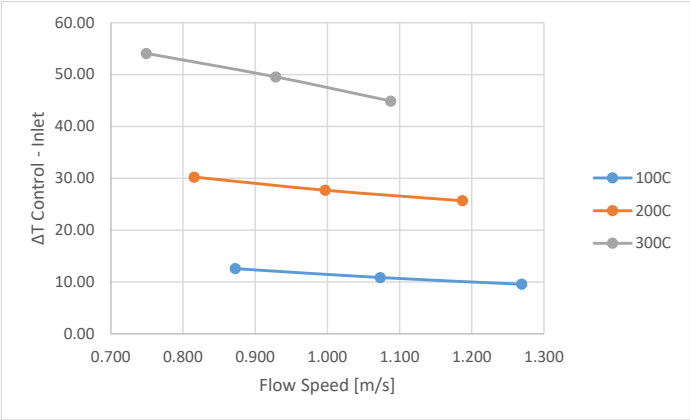

Fig. 7: Temperature lost between the Hotwind and the reactor (ΔT) at varying temperatures and flow rates.

The outlet TC is the second indicator of charge completion that results in a value of resident time (τ_{rT}) used for total charge energy. From Figure 5 it can be seen that the outlet TC values are the last to increase to values close to inlet temperature before equilibrating. However, unlike the mass data, the outlet temperature data has many points where the temperature has plateaued (ambient temperature, wet bulb temperature & final temperature). To work around this the 'end point' criteria is set to the last time gradient plateaus.

4.4. Energy Calculation.

Data collected from the CATS can now allow a calculation of charge energy for a material under the given drying conditions. Equation 2 highlights this:

$$Charge\ Energy\ (kJ) = \mu_{av} \times Cp \times \Delta T \times \tau_r \qquad \text{(eq. 2)}$$

- μ_{av} – Average Air Mass Flow [*kg/s*]
- Cp – Heat Capacity of Air [*kJ/KgK*]
- ΔT – Temperature Difference between Inlet and RT (25°C) [*K*]
- τ_r – Resident Time (Either based on Mass or Outlet Temperature) [*s*]

5. Results and Discussion

To assess the charge performance of silica gel, 1400g of discharged material was subject to three different temperatures (100°C, 200°C and 300°C) and various flow rates. The data received from Figure 7 was used to predict the temperature set at the Hotwind control TC to gain the desired inlet temperatures. For each temperature, 3 flow rates were chosen according to flow setting (Flow 4, Flow 7, and Flow 10) and 3 flow rates were chosen matching air mass flow values (20kg/hr, 25kg/hr, and 30kg/hr). This resulted in a total of 18 experiments shown in Figure 8.

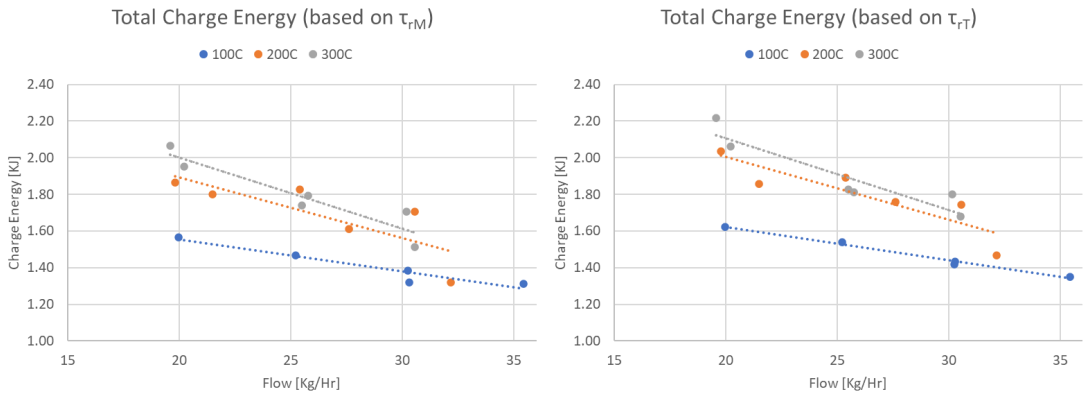

Fig. 8: Total energy to charge 1400g of fully discharged silica gel. Total charge energy based of τ_{rM} (Left). Total charge energy based of τ_{rT} (Right).

As mentioned above, there are two indicators of residence time (τ_r) which are mass and outlet temperature. The charge energy has therefore been calculated according to both values and presented on separate plots (Figure 8). Both sets of data show the same trends however the mass data generally gives slightly less energy values. This slight difference in τ_r values is due to fact that the mass data plateaus just before the outlet. Whereas the outlet temperature is a good indication of a complete reaction time, the mass data seems to slightly underestimate this. The rate of mass change towards the ends slows down before plateauing and exact final values is harder to identify. For this reason, outlet temperature can be considered a better indicator. Results show that an increase in flow rate and decrease in temperature leads to a reduced total charge energy and therefore a more efficient charge. The higher flow rates will allow easier removal of water vapor and the lower temperatures could suggest less heat energy is lost to the surroundings. If the reactor was better insulated this might improve the charge efficiency at elevated temperatures. This work suggests that if we have a waste heat source whereby we will capture that energy with silica gel, increasing the flow rate of that waste heat stream is more beneficial than maintaining higher temperatures. Additional fans or air supply could be considered for this.

The effect of material quantity on charge energy was assessed. Based on the previous study, the temperature was set at 100°C and three flow rates were selected (20kg/hr, 25kg/hr, and 30kg/hr). For each condition 6 mass values were chosen totaling 18 experiments shown in Figure 9.

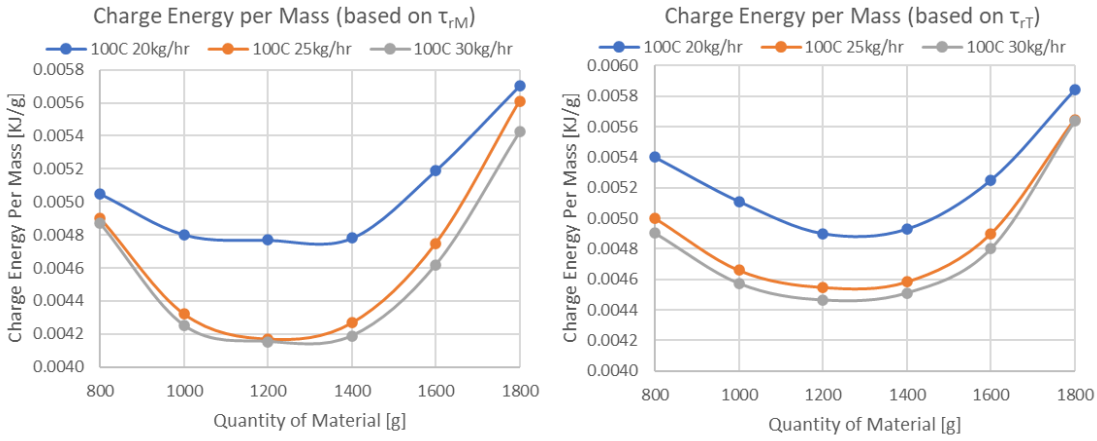

Fig. 9: Charge energy per mass for fully discharged silica gel. Charge energy based of τ_{rM} (Left). Charge energy based of τ_{rT} (Right).

Following the previous experiments, results are again presented on sperate plots whereby the charge energy per mass (kJ/g) was calculated based on τ_{rM} and τ_{rT}. As previously seen, the results based on mass data show slightly lower energy values. Whereas the trends observed are similar, the mass data is less consistent. The

data for outlet temperature is consistent between experiments (RT → Inlet Temp), whereas the mass change data varies due to there being varying mass changes. The mass gradient changes are less significant for the lower material quantities which might suggest the inaccuracy of this indicator at lower levels. However, the results show in both cases that there is an optimum material quantity around 1200g. Reduced efficiency before this value will be due to the energy lost in heating the reactor outweighing the energy used to charge to material. Reduced efficiency beyond this value would be due to reduced kinetics further up the reactor as more energy is being lost to the environment prior to the point. Figure 3 explains this by showing the reduced bulk 2 temperatures in comparison to bulk 1 (after a section is considered charged) that is further along the reactor. Again, better insulation could alleviate this problem allowing for better efficiency for higher material quantities. For a real-case heat capture solution, reactor material should be kept to a minimum and should be insulated as much as possible. To predict the best material quantity for any real-case, computational modelling should be done alongside this work where up-scaling can be easily considered.

6. Conclusion

The CATS has been developed and successfully demonstrated using silica gel as the commissioning material. It is predicted that maximum inlet temperatures of 530°C can be achieved using the Hotwind air flow system. Two indicators of residence time (mass and outlet temperature) have been used to calculate the total charge energy. Of the two, the outlet temperature data shows more consistent values and results that are a more accurate representation of a fully charged state. Total charge energy of silica gel has shown to decrease with higher flow rates and lower temperatures. In this case, 100°C was the lowest temperature applied. However, if silica gel is to be considered as a TCM, more work should be carried out at temperatures <100°C. The effect of material quantity on charge energy shows that there is an optimum quantity for silica gel in the reactor. The decrease in efficiency above 1200g is down to radiative heat loss increasing further up the reactor. Improvements in insulation properties should be considered to maintain efficiency at higher quantities. To predict the optimum quantity in real-case scenarios, future work on computational modelling will assist the transition from lab-scale to a full-scale demonstration. The CATS can now screen materials for their charge performance and make decisions on what material is best for real-case scenarios.

A synthesis protocol has also been developed for the consistent hydration of silica gel to hydration levels in the range of 33%, equivalent of a fully hydrated state. With use of the climate control oven, other materials that are capable of discharge within humid conditions (e.g. salt hydrates) could be successfully synthesized and analyzed for their charge performance in the CATS. Estimations of maximum inlet temperature indicate the possibility to study materials of higher charge temperature such magnesium hydroxide and calcium hydroxide.

7. References

BCS INC, 2008. Waste Heat Recovery: Technology & Opportunities in U.S. Industry. U.S. Department of Energy, Industrial Technologies.

Brueckner, S., Miró, L., Cabeza, L,F,. Pehnt, M., Laevemann, E., 2014. Methods to estimate the industrial waste heat potential of regions - A categorization and literature review. Renewable and Sustainable Energy Reviews. Elsevier. 38, 164–171. https://doi.org/10.1016/j.rser.2014.04.078.

Funayama, S., Takasu, H., Zamengo, M., Kariya, J., Kim, S., Kato, Y., 2019. Performance of thermochemical energy storage of a packed bed of calcium hydroxide pellet
s. Energy Storage. 1, e40. https://doi.org/10.1002/est2.40.

Fumey, B., Weber, R., and Baldini, L., 2019. Sorption based long-term thermal energy storage – Process classification and analysis of performance limitations: A review. Renewable and Sustainable Energy Reviews. Elsevier Ltd. 111, 57–74. https://doi.org/10.1016/j.rser.2019.05.006.

Krönauer, A., Lävemann, E., Brückner, S., Hauer, A., 2015. Mobile Sorption Heat Storage in Industrial Waste Heat Recovery. Energy Procedia. 73, 272-280. https://doi.org/10.1016/j.egypro.2015.07.688.

Lin, J., Zhao, Q., Huang, H., Mao, H., Liu, Y., Xiao, Y., 2021. Applications of low-temperature thermochemical energy storage systems for salt hydrates based on material classification: A review. Solar Energy. Elsevier Ltd. 214, 149–178. https://doi.org/10.1016/j.solener.2020.11.055.

Miró, L., Gasia, J., Cabeza, L.F., 2016). Thermal energy storage (TES) for industrial waste heat (IWH) recovery: A review. Applied Energy. 179, 284–301. https://doi.org/10.1016/j.apenergy.2016.06.147.

Papapetrou, M., Kosmadakis, G., Cipollina, A., La Commare, U., Micale, G, 2018. Industrial waste heat: Estimation of the technically available resource in the EU per industrial sector, temperature level and country. Appl. Therm. Eng. 138, 207-216. https://doi.org/10.1016/j.applthermaleng.2018.04.043.

Salviati, S., Carosio, F., Saracco, G., 2019. Hydrated salt/graphite/polyelectrolyte organic-inorganic hybrids for efficient thermochemical storage. Nanomaterials. 9, 420. https://doi.org/10.3390/nano9030420.

Sunku Prasad, J., Muthukumar, P., Densai, F., Basu, D,N., Rahman, M.M., 2019. A critical review of high-temperature reversible thermochemical energy storage systems. Applied Energy. Elsevier. 254, 113733. https://doi.org/10.1016/j.apenergy.2019.113733.

Sutton, R., Jewell, E., Elvins, J., Searle, J., Jones, P., 2018. Characterising the discharge cycle of CaCl2 and LiNO3 hydrated salts within a vermiculite composite scaffold for thermochemical storage. Energy Build. 162, 109-120. https://doi.org/10.1016/j.enbuild.2017.11.068.

TSI Airflow, 2014. Traversing a Duct to Determine Average Air Velocity or Volume. https://tsi.com/getmedia/1a11d344-0a58-4ca6-94fe-65721825686b/AF-106%20Traversing%20a%20Duct?ext=.pdf. Accessed July 2022.

Zamengo, M., Ryu, J., Kato, Y., 2015. Thermochemical performance of magnesium hydroxidee expanded graphite pellets for chemical heat pump. Energy Procedia. 71, 293-305. https://doi.org/10.1016/j.applthermaleng.2013.12.036.

Wu, H., Salles, F., and Zajac, J., (2019). A critical review of solid materials for low-temperature thermochemical storage of solar energy based on solid-vapour adsorption in view of space heating uses. Molecules. 24, 5. https://doi.org/10.3390/molecules24050945.